Spectroscopic study of the tunneling dynamics in N_2−water observed in the $O-D$ stretch region

R. Glorieux,[1] C. Lauzin,[1] A.J. Barclay,[2] M. Herman,[3] and N. Moazzen-Ahmadi[2]

[1)] *Institute of Condensed Matter and Nanosciences, Université catholique de Louvain (U.C.L.), Chemin du cyclotron, 2 1348 Louvain-la-Neuve, Belgium.*

[2)] *Department of Physics and Astronomy, University of Calgary, 2500 University Drive North West, Calagry, Alberta T2N 1N4, Canada.*

[3)] *Spectroscopy, Quantum Chemistry and Atmospheric Remote Sensing (SQUARES), Faculté des Sciences, Université libre de Bruxelles (ULB), 50 ave. F-D Roosevelt, B-1050, Brussels, Belgium.*

(Dated: 16 September 2021)

The $O-D$ stretch rovibrational spectra of N_2-D_2O and N_2-DOH were measured and analyzed. A combination band involving the in-plane N_2 bending vibration was also observed. These bands were recorded using a pulsed-slit supersonic jet expansion and a mid-infrared tunable optical parametric oscillator. The spectra were analyzed by considering the feasible tunneling motions and transitions were fitted to independent asymmetric rotors for each tunneling state. The rotational constants of the four tunneling components of N_2-D_2O were retrieved for the excited vibrational states. A two order of magnitude increase in the tunneling splittings is observed for the asymmetric $O-D$ stretch (ν_3 in D_2O) excitation compared to the symmetric stretch (ν_1 in D_2O) and to the ground vibrational state. This last finding indicates that the ν_3 vibrational state is likely perturbed by a combination state that include ν_1. Finally, the observation of a local perturbation in the ν_3 vibrational band, affecting the positions of few rovibrational levels, provides an experimental lower limit of the dissociation energy of the complex, $D_0 = 120$ cm^{-1}.

I. INTRODUCTION

Weakly bound water complexes containing atmospheric species is an extensive field of study for the understanding of radiative transfer budget[1,2] and chemistry occurring in the Earth's atmosphere[3–5].

The water-nitrogen is predicted as one of the most abundant dimer in the atmosphere[2,4,6,7] with a predicted partial pressure from $\sim 5.10^{-6}$ to 10^{-12} atm between the sea level and 25 km of altitude[2]. The N_2−water complex was the subject of numerous theoretical investigations[2,6,8–21] in the past four decades. In particular, Sadlej *et al.*[14] computed the global minimum structure of the complex and concluded that N_2-H_2O is planar with the N_2 monomer nearly colinear with the $O-H$ bond and gave an estimate for the interaction energy of $D_e = 403$ cm^{-1}. This value is close to the value obtained by Wheatley and co-workers[16] of $D_e = 441$ cm^{-1} which was determined from the evaluation of the intermolecular potential energy surface (PES) using a systematic intermolecular potential extrapolation routine. More recently, Barreto *et al.*[17] estimated a value of $D_e \sim 280$ cm^{-1} using the CCSD(T) method and an aug-cc-pVTZ basis sets. Using the same method extrapolated at the CBS limit, Ellington and Tschumper[19] found $D_e = 426.7$ cm^{-1}. The surface calculated by Wheatley and co-workers was later used by Wang and Carrington Jr[20] to evaluate the vibration-rotation-tunneling (VRT) energy levels of N_2-H_2O and N_2-D_2O. More recently, a new intermolecular PES averaged over the intramolecular Q_2 bending coordinate of the H_2O monomer was obtained at the CCSD(T)-F12a/aVTZ-bf level of approximation by Wang *et al.*[21]. They used their PES to reproduce microwave and infrared spectra of N_2-H_2O and N_2-D_2O and calculated dissociation energies (D_0) of 185.64 cm^{-1} and 221.18 cm^{-1}, respectively.

Experimentally, two high resolution microwave (MW) spectroscopic studies[22,23] of water-nitrogen complexes were reported in the literature. These studies showed that the N_2-D_2O complex is a near prolate top with an asymmetry parameter $\kappa \approx -0.9998$ and a large A rotational constant of ~ 11.5 cm^{-1}. The rotational energy levels are labelled by $J_{K_aK_c}$. As a result of the near prolate top structure of the complex, K_a is nearly a good quantum number and is highly significant. In the pioneer work of Leung *et al.*[22], $K_a = 0 \leftarrow 0$ rotational transitions were observed for several isotopologues. Stockman in his PhD thesis[23], reported the observation of $K_a = 0 \leftarrow 0$ transitions for N_2-H_2O and $K_a = 1 \leftarrow 0$ transitions for N_2-H_2O and N_2-D_2O. Analysis of the spectra of such complexes is challenging due to large amplitude motions of both water and nitrogen subunits that split each rotational level into four tunneling components. Indeed, four equivalent minima exist on the PES. The associated tunneling motions leads to a permutation of the two deuterium/hydrogen atoms (depending on whether N_2-D_2O or N_2-H_2O is considered), noted hereafter as $D-D$ or $H-H$ exchange and a concerted motion leading to the permutation of the two deuterium/hydrogen and the two nitrogen atoms noted in the rest of this paper as $N-N$ exchange.

Measurements have also been made in the mid-infrared (IR) region. The ν_2 bend region of water was studied by Springer *et al.*[24] for N_2-H_2O and by Zhu *et al.*[25] for N_2-D_2O. In both studies, the $H-H/D-D$ tunneling splitting was clearly resolved and the $K_a = 1 \leftarrow 0$, $K_a = 0 \leftarrow 0$ and $K_a = 0 \leftarrow 1$ subbands were observed and analyzed. Assuming a splitting independent of K_a (which we know is an assumption with a limited validity for similar complexes, i.e. CO−water[26]), Zhu *et al.*[25] determined the $D-D$ exchange tunneling splitting in the ground and excited vibrational states for both $K_a = 0$ and $K_a = 1$. They concluded that the $D-D$ exchange tunneling splitting decreases upon the excitation of the intramolecular

D_2O bending vibration ν_2 by about 26%. These results were reanalysed in the work of Wang and Carrington Jr[20]. These authors calculated the VRT levels in the ground vibrational state and determined that the splitting in $K_a'' = 0$ is about two times that for $K_a'' = 1$. Using these calculations and the assignments made by Zhu *et al.*[25], they concluded that the $D-D$ exchange tunneling splitting decreases upon the excitation of the D_2O bending vibration ν_2 by about 17% for $K_a' = 0$ states and by 32% for $K_a' = 1$ states compared to its value in the ground vibrational state.

This complex was also studied at lower resolutions in the infrared using helium nanodroplets[27,28] and rare gas matrices[29–31]. Two Fourier-Transform InfraRed (FTIR) spectroscopic studies investigated the effect of nitrogen adsorption on the $O-H(O-D)$ stretch of water clusters[14,32]. The interaction between N_2 and H_2O was also characterized by collisional cross section measurements using molecular beam scattering techniques[33]. In this report, the authors determined a value of 110 cm^{-1} for the dissociation energy, which is considerably smaller than the calculated values mentioned above.

In this work, the $a-$type $K_a = 0 \leftarrow 0$ and $b-$type $K_a = 1 \leftarrow 0$ rovibrational spectra of the $N_2 - D_2O$ complex in the ν_1 symmetric and ν_3 asymmetric $O-D$ stretch regions of D_2O are reported. The observation and the analysis of the intermolecular in-plane N_2 bend in the ν_3 asymmetric stretch region of D_2O in the complex is also presented. A global fit of the assigned transitions with all the previous microwave and infrared reported transitions is performed. A peculiar tunneling dynamics, with four series of well separated lines, is observed for the excited ν_3 asymmetric stretch and is discussed with regard to the observed spectra of $N_2 - D_2O$ around ν_1 and those for $N_2 - DOH$ in the $O-D$ stretch region. The remainder of the paper is organized as follows: Section II details the experimental methods and conditions, section III provides explanations concerning the selection rules, the model used to analyse the vibrational bands and subbands and the retrieved spectroscopic parameters. In section IV, we discuss the intermolecular dynamics of the complex and provide a lower limit for the dissociation energy (D_0). Concluding remarks are given in section V.

II. EXPERIMENTAL

The spectra were recorded at the University of Calgary using a rapid-scan tunable infrared continuous-wave optical parametric oscillator laser source to probe a pulsed supersonic slit jet expansion. The details of the experimental set-up and the data acquisition has been reported previously[34,35]. All the recorded spectra are shown in Fig. 1 along with the vibrational assignment. $N_2 - D_2O$ was formed in the supersonic jet expansion using N_2 and He bubbling through D_2O, except for the $K_a = 0 \leftarrow 0$ ν_3 band where a mixture of D_2O, N_2 and He was used. The backing pressure was typically in the range of 11-14 bar.

In the case of $N_2 - DOH$, HDO was formed by mixing D_2O and H_2O in the bubbler. By comparing the relative intensities of the simulated and observed spectra the rotational temperature of the complexes was found to be around 3 K.

III. SPECTRAL ASSIGNMENT AND ANALYSIS

Figure 2 presents a diagram of the VRT energy levels of $N_2 - D_2O$ drawn from the predictions of Wang and Carrington Jr[20] for the ground state (see Fig. 5 of Ref. 20, this choice is discussed further in section IV) and the energy levels structures for the ν_1 symmetric (left panel) and ν_3 asymmetric (right panel) $O-D$ stretch of D_2O (discussed further in section IV) from this work. The vertical arrows represent observed infrared transitions. Due to the $D-D$ and $N-N$ tunneling motions, the G_8 permutation inversion group (see Table 8 in Ref. 36) is the most relevant to label the VRT levels and the associated wavefunction. Considering the different degrees of freedom as decoupled, the ν_1 symmetric and ν_3 asymmetric stretches correspond respectively to the A_1^+ and B_1^+ irreducible representations in this group. The symmetry of the rotational wavefunction is characterized by the parity of K_a and K_c, and is A_1^+ if K_aK_c are respectively *even even* or *odd even* and A_1^- if K_aK_c are respectively *even odd* or *odd odd*. Concerning the tunneling components of the wavefunction, as reported in Ref. 20: "$A(B)$ indicate that a state is symmetric (anti-symmetric) with respect to the permutation of the two D atoms; the subscripts $1(2)$ indicate that a state is symmetric (anti-symmetric) with respect to the permutation of the two N atoms". In Fig. 2, the irreducible representation of the energy levels, obtained by a direct product of the vibrational, rotational and tunneling representations, is indicated. Considering that A_1^- is the irreductible representation of the electric dipole moment, selection rules are: $A_1^+ \leftrightarrow A_1^-$, $A_2^+ \leftrightarrow A_2^-$, $B_1^+ \leftrightarrow B_1^-$, $B_2^+ \leftrightarrow B_2^-$. The nuclear spin statistical weights of the VRT levels $A_1^{+/-}$, $A_2^{+/-}$, $B_1^{+/-}$, $B_2^{+/-}$ are indicated in parentheses and are respectively 4, 2, 2 and 1. To model and fit the measured experimental spectra, the standard S-reduced Watson asymmetric top Hamiltonian[37] was used and each tunneling state was fit independently. The expression of the Hamiltonian is [38]:

$$\begin{aligned}\hat{H}^{tun}(J) = {} & \nu_0 + A\hat{J}_z^2 + \overline{B}(\hat{\boldsymbol{J}}^2 - \hat{J}_z^2) + \frac{(B-C)}{4}(\hat{J}_+^2 + \hat{J}_-^2) \\ & - D_J\hat{\boldsymbol{J}}^4 - D_{JK}\hat{\boldsymbol{J}}^2\hat{J}_z^2 + d_1\hat{\boldsymbol{J}}^2(\hat{J}_+^2 + \hat{J}_-^2) \\ & + H_J\hat{\boldsymbol{J}}^6 + H_{JK}\hat{\boldsymbol{J}}^4\hat{J}_z^2,\end{aligned} \tag{1}$$

where the superscript ^{tun} refers to the vibration-tunneling component and $\overline{B} = \frac{B+C}{2}$. The analyses were performed using the PGOPHER software[39]. Due to the large A rotational constant, states with $K_a > 1$ were not sufficiently populated in the expansion and have thus not been observed.

The vibrational assignment, indicated in Fig. 1, was straightforward due to the proximity of the observed bands with the associated monomer mode frequency (D_2O or HDO). This was also made easier from the estimation of

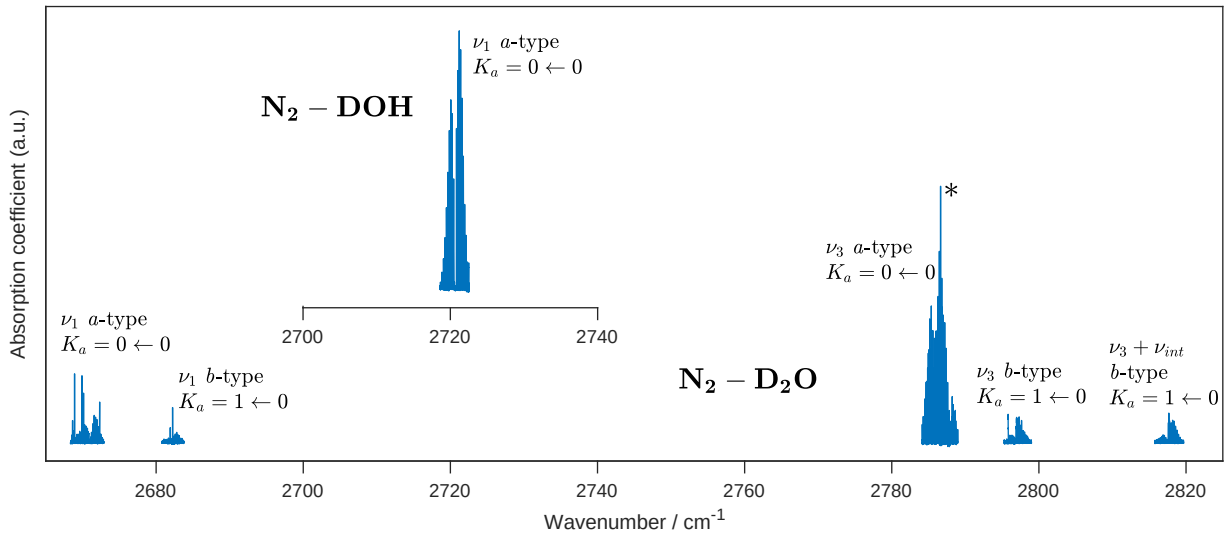

FIG. 1. Measured absorption spectra of $N_2 - D_2O$ and $N_2 - DOH$. The vibrational assignment is indicated next to each band. The intermolecular in-plane N_2 bending mode is noted here as ν_{int}. The relative intensity of the bands should be treated with caution due to variations in conditions of formation of the complex and laser intensity. This variation is outlined with an asterisk * for the ν_3 band measured using a gas mixture instead of bubbling Helium in D_2O as for the other bands.

the A rotational constant[23] and intermolecular modes frequencies[20] from previous studies. For the rotational assignment, ground state parameters were first fixed at the values obtained by Stockman [23] using the A-reduced Watson asymmetric top Hamiltonian for each tunneling state. Almost all the observed lines were assigned using the relative intensities dictated by the spin statistical weight and the temperature. Then a global fit of all the transitions reported in the millimeter-wave (mmW) by Stockman [23] and in the IR by Zhu *et al.* [25] with the assigned transitions from this work was performed using the standard S-reduced Watson asymmetric top Hamiltonian. This reduction is more appropriate for a near symmetric top[40]. Millimeter-wave transitions were given a weight 30 times larger than the weight of the IR transitions according to their respective experimental uncertainties. The weighted average error of the global fit was equal to 0.00058 cm^{-1}. The resulting $N_2 - D_2O$ ground state constants are reported in Table I while the refined ν_2 excited vibrational state constants can be found in Table S-20 of the supplementary materials[41].

A. Spectral assignment and analysis in the ν_1 symmetric stretch region

As shown in Fig. 3, only two subbands were observed in the ν_1 symmetric stretch region of D_2O, an a-type $K_a = 0 \leftarrow 0$ and a b-type $K_a = 1 \leftarrow 0$ subband. The two series of lines labelled by A and B correspond to the two tunneling components due to the $D - D$ exchange. In Fig. 3, the light blue subband belongs to the A tunneling component (degeneracy of A_1^+ and A_2^+ tunneling components) and the vermilion subband belongs to the B tunneling component (degeneracy of B_1^+ and B_2^+ tunneling components). The nuclear spin statistical weight equals 6 for A and 3 for B tunneling states. The assignment of the two subbands, the a-type and the b-type, was straightforward due to their well behaved relative intensities. As in ν_2, (see Fig. 2 of Ref. 25), no further splittings due to the $N - N$ permutation were observed. This splitting is also very small in the *G.V.S.* as indicated in the lower panel of Fig. 2.

In total, 76 transitions were assigned : 37/39 for the A/B tunneling component. The transition wavenumbers and their associated assignments are provided in Tables S-7 and S-8 of the supplementary materials[41]. The rotational constants for the excited vibrational state ν_1 from this analysis and the global fit are reported in Table II. Because of the resolution and the congestion of the Q-branch in the $K_a = 1 \leftarrow 0$ spectrum, some Q transitions remain unassigned especially for the A tunneling component.

B. Spectral assignment and analysis in the ν_3 asymmetric stretch region

The experimental $K_a = 0 \leftarrow 0$ spectrum in the excited ν_3 vibrational state is shown in the bottom panel of Fig. 4. There is a stark contrast between the $K_a = 0 \leftarrow 0$ bands of the ν_1 (lower panel of Fig. 3) and the ν_3 fundamental (bottom panel of Fig. 4). Indeed, the $K_a = 0 \leftarrow 0$ band of the ν_3 fundamental consists of four rotational series, rather than two for the $K_a = 0 \leftarrow 0$ of the ν_1 fundamental. These can be assigned to the four tunneling components A_1^+, A_2^+, B_1^+, B_2^+ based on relative intensity of the theoretical spin statistical weights. The assignment for the VRT components $A_2^{+/-}$ and $B_1^{+/-}$ having the same nuclear spin statistical weight (2) was made using the lower state combination differences from the mmW work by Stockman [23].

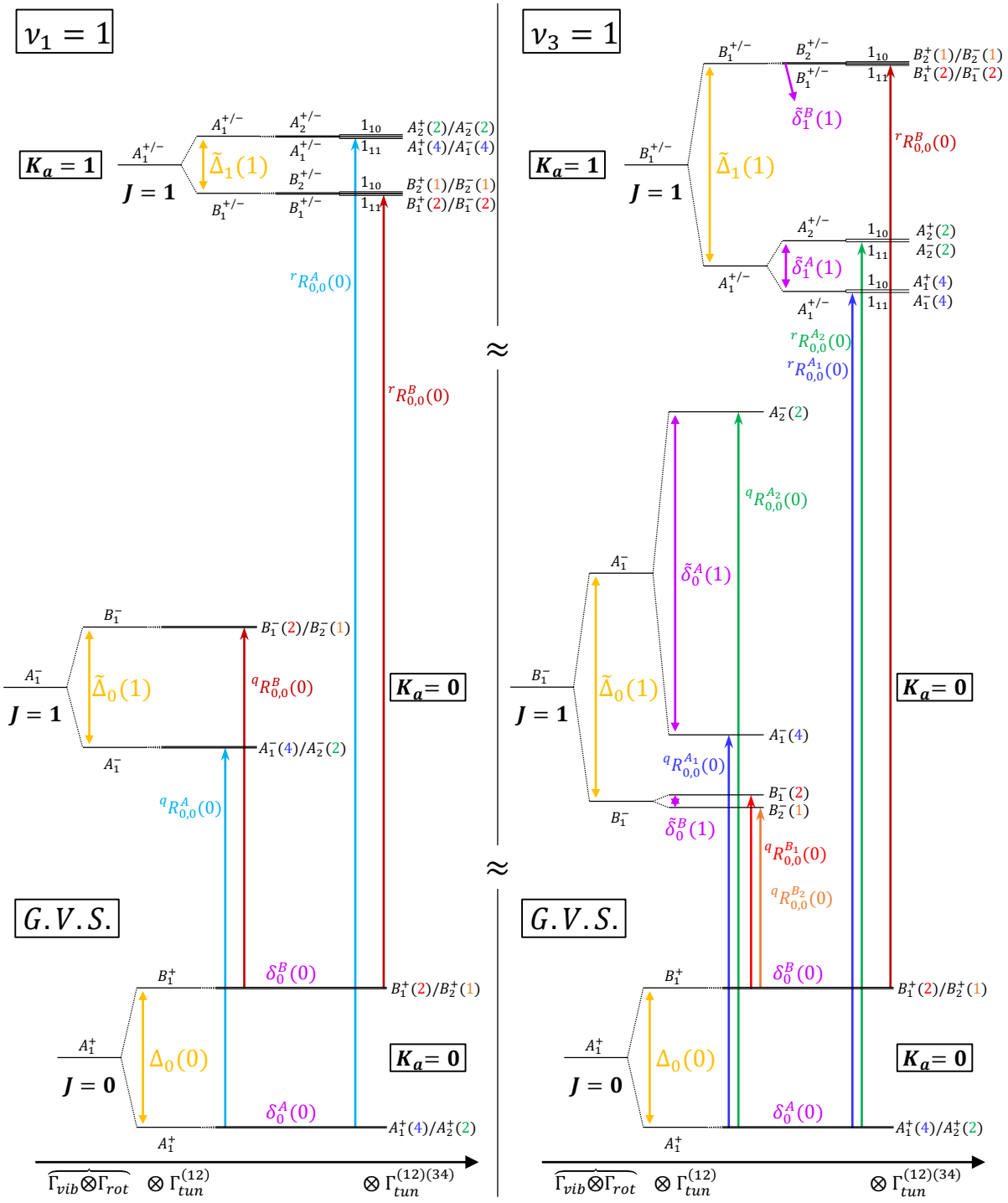

FIG. 2. Schematic representation of the vibration-rotation-tunneling energy levels with their respective irreducible representation in G_8 and spin statistical weight of the $N_2 - D_2O$ complex in the ground vibrational state *G.V.S.* (from Ref.[20]), in the $\nu_1 = 1$ symmetric stretch region (left panel) and in the $\nu_3 = 1$ asymmetric stretch region (right panel) of the D_2O monomer (from this work). All the splittings are plotted at the same scale. The asymmetry splitting for $K_a = 1$ states has the same order of magnitude as the N – N exchange tunneling splitting for $J = 1$. The D – D and N – N exchange tunneling splitting are noted as $\Delta_{K_a}(J)$ and $\delta_{K_a}^{A/B}(J)$, respectively. The tilde '$\sim$' indicates the splittings in the excited vibrational states. The vertical arrows represent the observed transitions from this work. Transitions are labelled with ${}^{\Delta_{K_a}}\Delta J^{tun}_{K_a'',K_c''}(J'')$, where the superscript ^{tun} refers to the initial VRT component with A/B referring the degeneracy of A_1^+/B_1^+ and A_2^+/B_2^+ tunneling components. The double tilde '$\approx$' indicates changes of the vertical energy scale which applies also to the arrows representing observed transitions.

Observation of four $K_a = 0 \leftarrow 0$ subbands for the ν_3 fundamental was unexpected. This is in stark contrast with the ν_1

TABLE I. Molecular constants (in cm^{-1}) [a] for the ground vibrational state of the $N_2 - D_2O$ complex.

	Ground vibrational state			
	$A_1^{+/-}$	$A_2^{+/-}$	$B_1^{+/-}$	$B_2^{+/-}$
A	11.4957522(96)	11.4953804(96)	11.167868(22)	11.167940(22)
B	0.0932485(30)	0.0932439(30)	0.0930529(73)	0.0930494(75)
C	0.0919477(15)	0.0919457(15)	0.0920307(39)	0.0920288(40)
$10^3 D_{JK}$	-0.47148(67)	-0.47355(67)	-0.50604(96)	-0.50596(97)
$10^6 D_J$	1.033(13)	1.026(13)	1.014(25)	1.003(25)
$10^6 d_1$	-0.0441(67)	-0.0428(67)	-0.0388(74)	-0.0359(75)
$10^6 H_{JK}$	-0.1830(74)	-0.1861(74)	-0.1765(77)	-0.1772(78)

[a] Numbers in parentheses are the uncertainties and are in the same units.

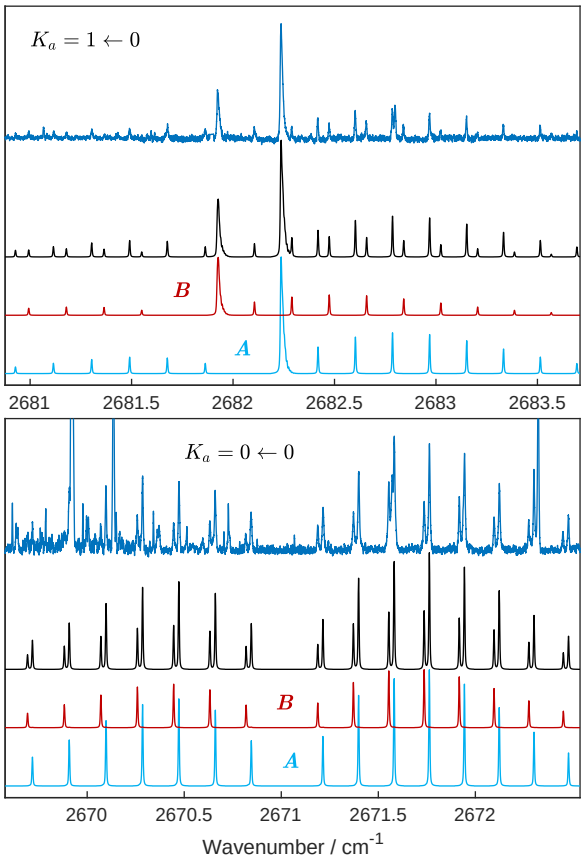

FIG. 3. Spectra of the $N_2 - D_2O$ complex in the ν_1 symmetric stretch region of D_2O. The upper panel shows the fundamental *b*-type $K_a = 1 \leftarrow 0$ band and the lower panel shows the fundamental *a*-type $K_a = 0 \leftarrow 0$ band. In each panel the observed spectrum is depicted in blue and the black trace is the sum of the simulated spectra of the different tunneling components. The unassigned high intensity transitions are probably due to the D_2O dimer while the unassigned low intensity transitions could belong to larger complexes.

spectra from this work and previously reported spectra in the infrared which either did not show any $N-N$ tunneling splitting[25] or the $N-N$ tunneling splitting, for ν_2 in the case of $N_2 - H_2O$[24], was at least an order of magnitude smaller. This observation can be rationalized in terms of $D-D$ and $N-N$ tunneling splittings and is a signature of a large change of the intermolecular dynamics in the ν_3 region, as further discussed in section IV.

In addition, the $K_a = 1 \leftarrow 0$ subband was measured in the asymmetric stretch region of D_2O for both the fundamental and the in-plane N_2 bending intermolecular mode. These bands are shown in the middle and top panels of Fig. 4, respectively. To fit the combination band involving an intermolecular mode, the *A* rotational constant was fixed to its value for the ν_3 fundamental as it can not be determined from the observation of this band alone. In both spectra, the $N-N$ tunneling splitting was resolved for the *A* tunneling states. This splitting was on the other hand only resolved in the *B* tunneling states for the combination band. Again, the distinction between the $A_2^{+/-}$ and $B_1^{+/-}$ components was determined by using the lower state combination differences. The assignment of the *b*-type fundamental and intermolecular mode bands was straightforward thanks to the previous assignment of the *a*-type fundamental, except for the $A_2^{+/-}$ subband of the intermolecular mode, for which the *Q*-branch is shaded to blue for the first few lines and folds back on itself at ${}^rQ_{0,6}(6)$. This unexpected behavior is discussed in section IV.

Transitions marked with an asterisk in Fig. 4 are the perturbed transitions. These lines indeed have an observed minus calculated value at least two times higher than the root-mean-square (RMS) deviation of the global fit. They were, therefore, excluded from the final fit. The origin of the pertubations is discussed in the next section. The remaining unassigned transitions could belong to an intermolecular mode of $N_2 - D_2O$ associated with ν_1 or due to other complexes. In total, 154 transitions were assigned in the ν_3 fundametal bands and 95 in the combination band. The observed transitions and their assignment are available in Tables S-9 to S-16 of the supplementary materials[41]. The rotational constants for the excited vibrational states ν_3 and $\nu_3 + \nu_{int}$ from this analysis and the fit are reported in Tables III and IV, respectively.

TABLE II. $N_2 - D_2O$ molecular constants (in cm^{-1}) [a] for the (ν_1) symmetric O − D stretch vibrational state.

	Excited state ν_1			
	$A_1^{+/-}$	$A_2^{+/-}$	$B_1^{+/-}$	$B_2^{+/-}$
ν_0	2671.03083(27)	2671.03083(27)	2671.00342(26)	2671.00341(26)
A	11.29493(36)	11.29492(36)	11.00955(31)	11.00954(31)
B	0.092901(17)	0.092897(17)	0.092782(16)	0.092779(16)
C	0.091469(17)	0.091466(17)	0.091530(18)	0.091528(18)
$10^3 D_{JK}$	-0.5132(99)	-0.5135(99)	-0.5421(87)	-0.5421(87)
$10^6 D_J$	1.11(12)	1.10(12)	1.25(13)	1.24(13)

[a] Numbers in parentheses are the uncertainties and are in the same units.

TABLE III. $N_2 - D_2O$ molecular constants (in cm^{-1}) [a] for the (ν_3) asymmetric O − D stretch vibrational state.

	Excited state ν_3			
	$A_1^{+/-}$	$A_2^{+/-}$	$B_1^{+/-}$	$B_2^{+/-}$
ν_0	2785.95164(44)	2786.43729(36)	2785.62834(29)	2785.60951(34)
A	11.07629(55)	10.67494(50)	11.53919(41)	11.55802(46)
B	0.090858(55)	0.093977(57)	0.092759(37)	0.092765(47)
C	0.087490(55)	0.092843(57)	0.090087(37)	0.090093(47)
$10^3 D_{JK}$	-4.215(54)	0.159(53)	-2.527(29)	-2.519(42)
$10^6 D_J$	-20.1(12)	-4.2(11)	4.95(16)	0.94(64)
$10^6 d_1$	-2.55(12)	7.22(34)	-3.56(33)	-3.57(33)
$10^6 H_{JK}$	-21.5(12)	-1.5(11)	1.22(42)	-2.78(75)

[a] Numbers in parentheses are the uncertainties and are in the same units.

TABLE IV. $N_2 - D_2O$ molecular constants (in cm^{-1})[a] for the excited state $\nu_3 + \nu_{int}$.

	Excited state $\nu_3 + \nu_{int}$			
	$A_1^{+/-}$	$A_2^{+/-}$	$B_1^{+/-}$	$B_2^{+/-}$
ν_0	2806.62345(30)	2807.12446(35)	2806.29151(32)	2806.28807(29)
A [b]	11.07629	10.67494	11.53919	11.558016
B	0.096028(36)	0.085398(63) [c]	0.095961(47)	0.095616(50)
C	0.093341(37)	0.094287(67) [c]	0.094914(50)	0.093355(34)
$10^6 D_J$	3.24(73)	-44.6(20)	3.5(12)	-5.10(44)
$10^6 d_1$	0.16(13)	28.7(25)	15.71(21)	-3.06(34)
$10^9 H_J$	15.7(47)	-50(18)	78.3(93)	

[a] Numbers in parentheses are the uncertainties and are in the same units.
[b] The A rotational constant was fixed to its value for the ν_3 excited state for each tunneling state during the fit.
[c] The effective B rotational constant is smaller than the C rotational constant. This result is discussed in section IV.

IV. DISCUSSION

Perturbations and interaction energy

By observing discrete perturbations in water-carbon monoxide spectra and by assigning the vibrational level of the perturbing state, Barclay *et al.* [26] obtained an experimental lower limit for the binding energy D_0 of the $D_2O - CO$ complex. We also observed discrete perturbations for $N_2 - D_2O$. This is not surprising due to isoelectronicity with $D_2O - CO$. Therefore, we performed a similar analysis to find a lower limit to the binding energy of $N_2 - D_2O$.

In Fig. 4, seven perturbations were identified and marked with asterisks on the unperturbed locations: three for the $A_1^{+/-}$ subband (bottom panel) and four for the $A_2^{+/-}$ subband (top and bottom panels). The transitions marked with the same symbol are transitions reaching the same ν_3 $J'_{K'_a K'_c}$ energy level. The two most perturbed transitions in this band are illustrated in panels (b) and (c) of Fig. 5. Here panel (a) shows a portion of the measured and simulated spectra for a regular set of lines and panels (b) and (c) illustrate the two perturbed lines having the same upper state, namely $J' = 7$ whose energy is at 2791 cm^{-1}. These transitions were assigned using lower state combination differences and considering an experimental accuracy of 0.0005 cm^{-1}. As expected, the difference between the observed and calculated transitions for the two transitions

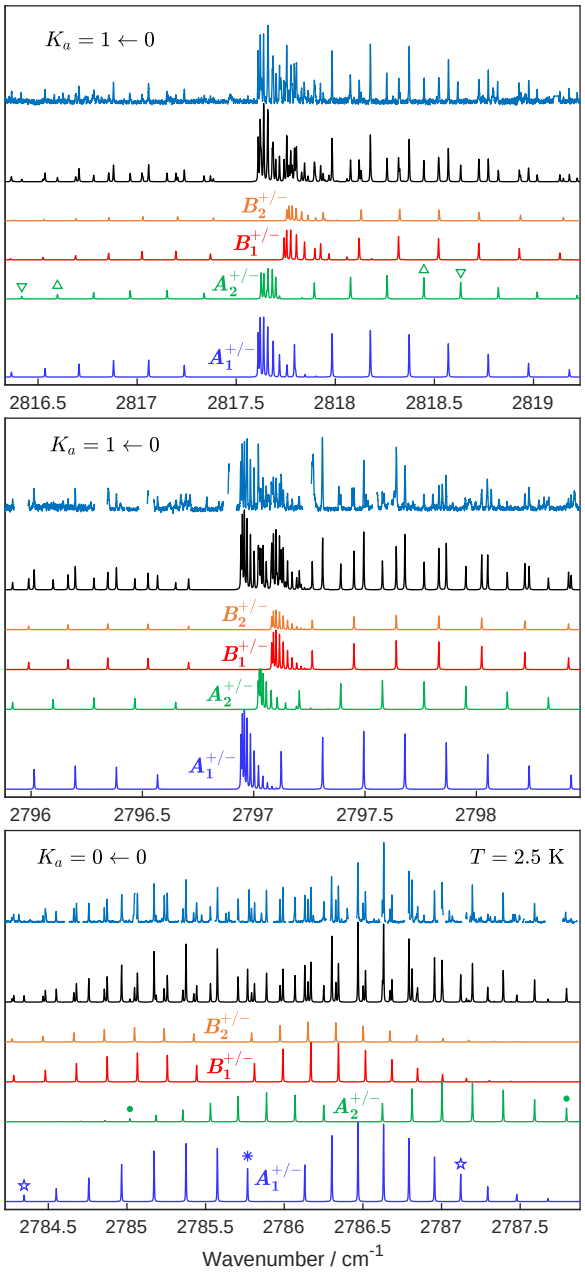

FIG. 4. Spectra of the $N_2 - D_2O$ complex in the ν_3 asymmetric stretching region of D_2O. The top panel shows the *b*-type $K_a = 1 \leftarrow 0$ combination band, the middle panel shows the fundamental *b*-type $K_a = 1 \leftarrow 0$ band and the bottom panel shows the funcamental *a*-type $K_a = 0 \leftarrow 0$ band. The top blue spectrum in each panel is the observed one and the black simulated spectrum represents the sum of the contributions of the $A_1^{+/-}$ (blue), $A_2^{+/-}$ (green), $B_1^{+/-}$ (red) and $B_2^{+/-}$ (orange) VRT components. Transitions marked by $\triangledown, \triangle, \star, \bullet, *$ are perturbed and lines marked with the same symbol reach the same $J'_{K'_aK'_c}$ level. Gaps in the measured spectra are transitions present when the expansion mixture consists of D_2O and He only.

is the same and about 0.071 cm^{-1}. We observe similar behavior for $P(8)$ and $R(6)$ of the $A_2^{+/-}$ subband.

The nearest perturbing vibrational state is the ν_1 symmetric stretch of D_2O with a band origin located at 2671 cm^{-1}. This value is computed from this work assuming the same vibrational shift as for ν_3. The next nearest perturbing monomer vibrational states are the $\nu_2 = 2$ bends of D_2O at 2337 cm^{-1}[42] and the stretch of N_2 calculated at 2359 cm^{-1} for $N_2 - H_2O$ by Ellington and Tschumper[19].

The latter two candidate states can be ruled out since they result in a lower bound dissociation energy of 454 or 432 cm^{-1}. These are very close to the interaction energy $D_e =$ 441 cm^{-1}[16]. Note that the zero point energy for $N_2 - D_2O$ is calculated to be 232 cm^{-1}[20].

The other possibility for the source of perturbation is a vibrational state with one quantum of excitation of ν_1 in combination with an intermolecular mode. The support for this assumption comes from the work by Wang and Carrington Jr.[43] who predict a large density of intermolecular modes between 90 cm^{-1} and 130 cm^{-1}. This yields an experimental value of $D_0 > 120$ cm^{-1}. This lower bound limit is consistent with D_0 of 209 cm^{-1} obtained from the interaction energy of 441 cm^{-1} and zero point energy of 232 cm^{-1} and also consistent with the dissociation energy of 221.18 cm^{-1} calculated by Wang *et al.*[21]. It also rules out the value of $D_e = 110$ cm^{-1} obtained from the molecular scattering experiment[33].

The rotational constants in $\nu_3 + \nu_{int}$

The molecular constants of the excited $\nu_3 + \nu_{int}$ vibrational state are presented in Table IV and the associated simulation is illustrated in the upper panel of Fig. 4. One surprising result from our fit is that the *B* rotational constant is smaller than *C* for the $A_2^{+/-}$ VRT component. This can be explained by the reversal of energy ordering of the asymmetry doublets for $K_a = 1$. Such a reversal have already been observed for $K_a = 2$ in the $CO - Ar$[44] and the $Ar - HCCH$[45,46] complexes. Following these authors, the asymmetry splittings term for $K_a = 1$ can be expressed as[47,48]:

$$\Delta E(K_a = 1) = \frac{(B-C)}{2} J(J+1) + 2d_1 J^2 (J+1)^2. \quad (2)$$

Our experimental rotational constants, where $B < C$, is simply a reflection of reversal of energy ordering for $K_a = 1$ which are due to vibrational perturbations as in $CO - Ar$[44] or the limitations of the semi-rigid Hamiltonian to describe a floppy molecule.

The perturbation of the $K_a = 1$ $A_2^{+/-}$ levels is likely due to the $K_a = 2$ levels of the ν_3 vibrational state. Indeed, in the ground vibrational state[20], the $K_a = 2$ levels are predicted to be approximately 4.6 cm^{-1} higher than the considered intermolecular mode wavenumber.

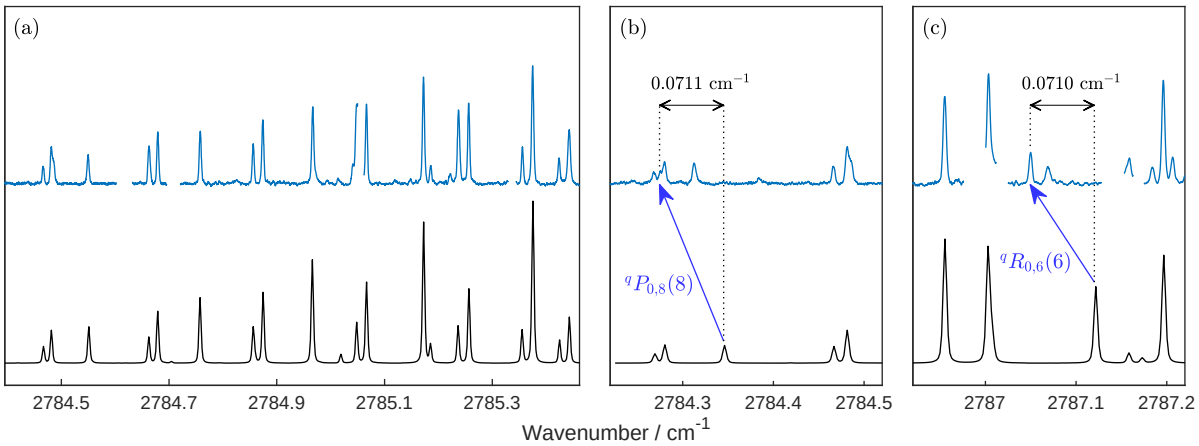

FIG. 5. Small sections of the ν_3 $K_a = 0 \leftarrow 0$ subband with the observed spectra in blue and the simulated spectra in black. The left panel illustrates the good agreement between the simulated and observed spectra. Panels (b) and (c) illustrate perturbed transitions for the $A_1^{+/-}$ VRT component : these are connected to their experimental positions by a blue arrow.

The dependency of the intermolecular dynamics with rovibrational excitation

We are interested in the tunneling dynamics and its dependence on vibrational and rotational excitation. Experimentally, the observation of high resolution spectra gives only access to the sum (or difference) between the excited and ground state splittings. To infer information on the dependence of the tunneling splittings on the vibrational and rotational excitation, we will use as a reference the theoretical energy levels from Ref. 20 for the ground vibrational state.

To test the validity of the approach and the quality of the calculations performed in Ref. 20, the predicted in-plane N_2 bending intermolecular mode wavenumber can be compared to our experimental value. We observed $K_a = 1 \leftarrow 0$ transitions reaching the $\nu_3 + \nu_{int}$ vibrational state. From Eq. 1 and Table IV, the measured origin of the mode can be evaluated for $J = 1$ and $K_a = 1$ using $\nu_0^{\nu_3+\nu_{int}} + A + \bar{B} - \nu_0^{\nu_3}$. This gives : 31.843, 31.452, 32.298 and 32.331 cm^{-1}, for the $A_1^{+/-}$, $A_2^{+/-}$, $B_1^{+/-}$ and $B_2^{+/-}$ tunneling states, respectively. The difference with theoretical predictions are: -0.643, -0.149, 0.185 and 0.216 cm^{-1}. Taking into account a variation smaller or of the order of 1 cm^{-1} due to the asymmetric stretch excitation of water in the complex compared to the theoretical values which are for the ground vibrational state, the calculated values can be considered as excellent[20].

By using the reported origin of each tunneling state for the ground vibrational state[20], the amplitude of the splittings in the ground vibrational state were obtained. These are reported in Table S-21[41]. By using the calculated values of the splittings in the ground vibrational state, the assigned transitions observed in ν_2[25] and the observed transitions in this work, the splittings in the ν_2, ν_1, ν_3 and $\nu_3 + \nu_{int}$ vibrational states were estimated. The values of the splittings in each vibrational state are reported in Tables S-22 to S-24[41] for several J values along with the procedure followed for their evaluation. Table V gives these splittings for $J = 1$.

From examination of Table V, we find that the $D-D$ exchange tunneling splitting in the ν_2 and ν_1 vibrational excited states (the $N-N$ tunneling splitting is not resolved in these states) are nearly identical and slightly smaller than in the ground vibrational state. In addition, there is a decrease of the tunneling splitting with K_a. This has been interpreted as a K_a dependent tunneling barrier, where the K_a rotational excitation about the inter-monomer axis pushes the minima of the effective PES appart[20]. In the ν_3 excited vibrational state, however, the results are very surprising. As evaluated from Table V, the $D-D$ exchange tunneling splitting increases from its *G.V.S.* value by about 62 % and nearly 200 % for $K_a = 0$ and 1, respectively. Secondly, the $N-N$ exchange tunneling splitting for $K_a = 0$ increases by two orders of magnitude or more. This splitting in the B states is ± 217 times and in the A states is ± 3522 times its value in the *G.V.S.* (see right panel of Fig. 2). For $K_a = 1$, the $N-N$ tunneling splitting in the A states is ± 361 times greater. Eventhough this splitting in the B tunneling states was not resolved, it was calculated (see the supplementary materials[41]).

As illustrated in Tables S-21 to S-24[41], we also observe a dependence of the tunneling ($D-D$ and when observed $N-N$) splitting with J. This dependence differs according to the excited vibrational state and K_a excitation. For $K_a = 0$, a small decrease of the $D-D$ tunneling splitting with J in the ground, ν_2 and ν_1 vibrational states is observed while there is a larger decrease in the ν_3 vibrational excited state. For $K_a = 1$, the $D-D$ tunneling splitting increases rapidly with J in the ν_2 and ν_1 vibrational states, highlighting the same behavior for these two vibrational states. Finally, the tunneling splittings in the ν_3 vibrational excited state and in the combination mode $\nu_3 + \nu_{int}$ are also similar for $J = 1$ and $K_a = 1$. However this dependence in the combination mode changes much stronger (i.e. between $J = 1$ and $J = 7$, $\tilde{\Delta}_1(J)$ increases by ± 30 %, $\tilde{\delta}_1^A(J)$ and $\tilde{\delta}_1^B(J)$ decreases by about 120 % and

TABLE V. Calculated exchange tunneling splittings for $J = 1$ in the ground vibrational state *G.V.S.* and in the excited ν_2, ν_1, ν_3 and in $\nu_3 + \nu_{int}$ vibrational states of the $N_2 - D_2O$ complex due to the $D - D$ tunneling motion ($\Delta_{K_a}(J)$) and to the $N - N$ tunneling motion ($\delta^{A/B}_{K_a}(J)$) in the complex (a tilde '$\sim$' is added to indicate the excited vibrational states splittings). The detailed calculations can be found in the supplementary materials[41]. Values of the exchange tunneling splitting are expressed in (cm^{-1}) and rounded to four significative digits after the decimal place for Δ and five for δ.

	Exchange tunneling splittings					
	$K_a = 0$			$K_a = 1$		
	$\Delta_0(1)$	$\delta^A_0(1)$	$\delta^B_0(1)$	$\Delta_1(1)$	$\delta^A_1(1)$	$\delta^B_1(1)$
in the *G.V.S.*	0.2201 [a]	0.00014 [a]	0.00009 [a]	0.1075 [a]	0.00022 [a]	0.00017 [a]
	$\tilde{\Delta}_0(1)$	$\tilde{\delta}^A_0(1)$	$\tilde{\delta}^B_0(1)$	$\tilde{\Delta}_1(1)$	$\tilde{\delta}^A_1(1)$	$\tilde{\delta}^B_1(1)$
in ν_2	0.1825 [b]			0.0754 [b]		
in ν_1	0.1930			0.1076		
in ν_3	0.3560	0.4931	0.0195	0.3190	0.0795	0.0031
in $\nu_3 + \nu_{int}$				0.3108	0.0961	0.0154

[a] Computed from Ref. 20, 23, and 25, this work and the PGOPHER software[39].
[b] Computed using observed transitions from Ref. 25.

250 % in the combination mode, respectively while $\tilde{\Delta}_1(J)$ increases by 6.1 % and $\tilde{\delta}^A_1(J)$ decreases by 9.9 % in the ν_3 fundamental). As before, the result in the excited ν_3 vibrational state (and in the combination mode $\nu_3 + \nu_{int}$) are unexpected and different from all other studied vibrational states.

To explain the observed differences of the intermolecular dynamics in the ν_3 region compared to the other vibrational states, several mechanisms were considered. The more likely explanation is that the ν_3 mode is mixed with one (or more) dark background state(s) involving one or several N_2 bending excitation. Multiple excitation of such mode would significantly promote the $N - N$ interchange as observed here. There could be multiple coincidences, say a different dark vibrational state for each of the three bands observed in the ν_3 region, but this is not required and there needs to be only one such perturbing state whose zero-order vibrational frequency happens to lie very close to that for ν_3 vibrational state. This is because ν_3 has large splittings but these splittings are different for $K_a = 1$ and the combination band. The less likely possibility is that the ν_3 intramolecular vibrational excitation decreases the potential energy barrier between minima on the PES, increasing the amplitude of the tunneling splittings in this excited vibrational state.

In order to rule out any fundamental change of the PES topology induced by intramolecular vibrational excitation and gain experimental insight on the tunneling dynamics in ν_3, the $K_a = 0 \leftarrow 0$ spectrum of $N_2 - DOH$ in the $O - D$ stretch region (called ν_1 hereafter, following the isolated DOH nomenclature) has been measured. In this complex, hydrogen atoms are not identical and a nuclear permutation leads to two different isomeric species, i.e. $N_2 - DOH$ and $N_2 - HOD$. The ground state combination differences from the mmW spectra[23] ensured that the observed band belongs to the $N_2 - DOH$ complex. Again, a global fit was performed by fitting both the mmW transitions[23] and the IR transitions from this work with a weight 30 times larger for the mmW transitions. The observed mmW $^rR_{0,0}(0)$ transition was not included in the fit due to its large experimental uncertainty. The resulting ground and excited ν_1 vibrational states molecular constants can be found in Tables VI and VII, respectively. The weighted average error of this global fit was equal to 0.00037 cm^{-1}.

TABLE VI. $N_2 - DOH$ molecular constants (in cm^{-1}) [a] for the ground vibrational state.

	Ground vibrational state	
	$A_1^{+/-}$	$A_2^{+/-}$
A	17.4707240(66)	17.4711141(66)
B	0.0968095(12)	0.09681043(80)
C	0.0956351(11)	0.09563414(93)
$10^3 D_{JK}$	-1.72792(40)	-1.72584(38)
$10^6 D_J$	1.179(15)	1.1619(49)
$10^6 d_1$	-0.0759(43)	-0.0729(43)
$10^6 H_{JK}$	-0.4211(51)	-0.4215(50)
$10^9 H_J$	0.127(68)	

[a] Numbers in parentheses are the uncertainties and are in the same units.

TABLE VII. $N_2 - DOH$ molecular constants (in cm^{-1}) [a] for the ν_1 vibrational state.

	Excited state ν_1	
	$A_1^{+/-}$	$A_2^{+/-}$
ν_0	2720.63798(18)	2720.63798(18)
A [b]	17.4707240	17.4711141
$\bar{B}$	0.0954850(93)	0.0954859(93)
$10^6 D_J$	1.118(86)	1.124(86)

[a] Numbers in parentheses are the uncertainties and are in the same units.
[b] The A rotational constant was fixed to its ground state value for each tunneling state during the fit.

The assignment of the $K_a = 0 \leftarrow 0$ $N_2 - DOH$ spectrum in the ν_1 excited vibrational state was straightforward because of a clear rotational structure as well as the absence of any

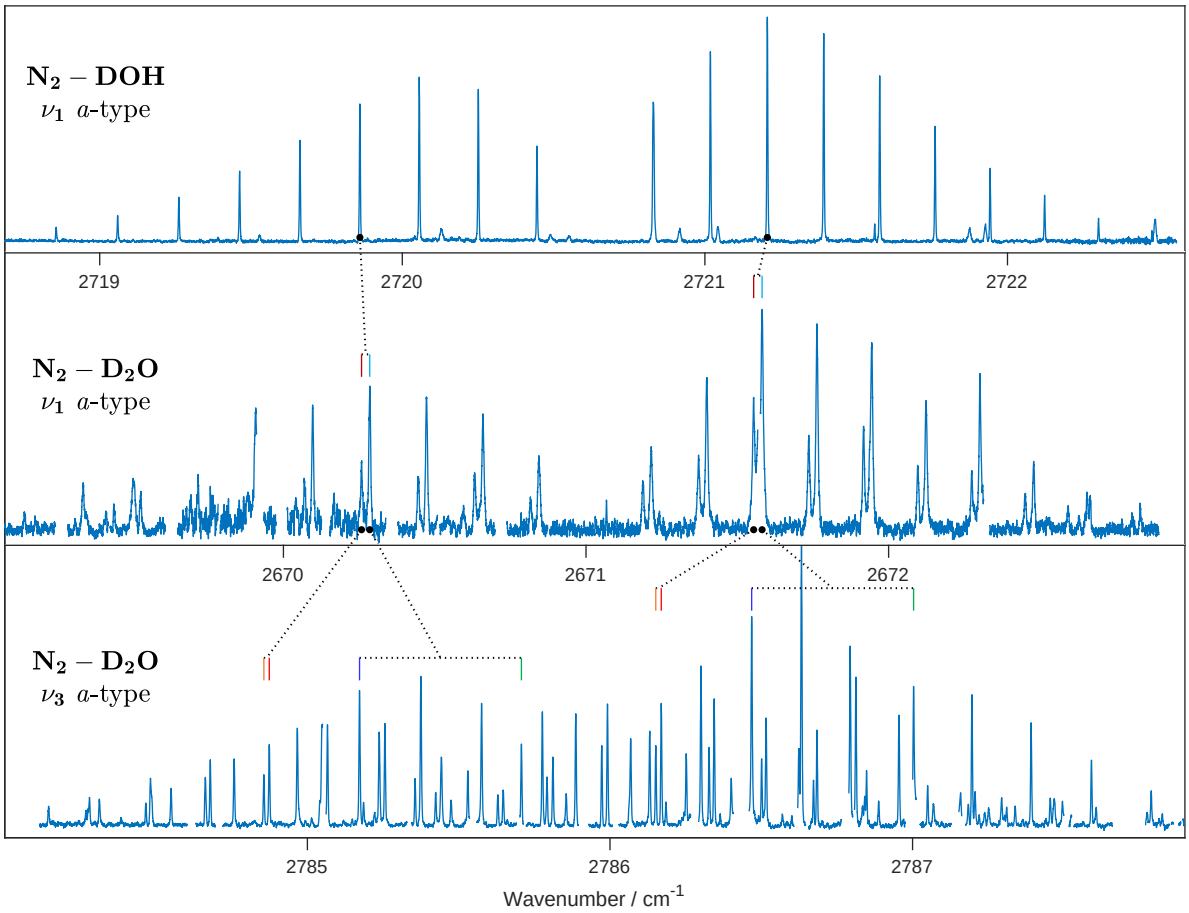

FIG. 6. Measured $N_2 - DOH$ and $N_2 - D_2O$ a-type $K_a = 0 \leftarrow 0$ spectra. The top panel shows the a-type $K_a = 0 \leftarrow 0$ spectrum of $N_2 - DOH$ in the excited $O - D$ stretching region, the middle panel shows the a-type $K_a = 0 \leftarrow 0$ spectrum of $N_2 - D_2O$ in the excited ν_1 symmetric stretch of D_2O and the bottom panel shows the a-type $K_a = 0 \leftarrow 0$ spectrum of $N_2 - D_2O$ in the excited ν_3 asymmetric stretch of D_2O. From top to bottom, the colored bars show the evolution of the ${}^qP_{0,4}(4)$ and ${}^qR_{0,2}(2)$ lines splitting firstly due to the $D - D$ exchange tunneling motion and secondly due to the concerted motion leading to the $N - N$ permutation. The blank regions in the spectrum of $N_2 - D_2O$ in the ν_1 symmetric stretch region are unassigned transitions not shown for more clarity.

tunneling splitting. The measured spectrum is shown in the top panel of Fig. 6.

Figure 6 illustrates the evolution of the tunneling splittings in the $O - D$ stretch regions of the water molecule for $N_2 - DOH$ and $N_2 - D_2O$. The top panel shows the $N_2 - DOH$ spectrum in the $O - D$ asymmetric stretch region, the middle and bottom panels show the $N_2 - D_2O$ spectrum in the $O - D$ symmetric and asymmetric stretching regions, respectively. The dotted lines linking the spectra show the evolution of the tunneling splittings of the ${}^qP_{0,4}(4)$ and ${}^qR_{0,2}(2)$ transitions. The lines connecting top and middle panels show the doubling due to the $D - D$ exchange and the lines connecting the middle to the bottom panels show an additional doubling due to the concerted motion of the water and nitrogen subunits leading to both the $D - D$ and $N - N$ permutation. This figure highlights the energy levels structures found in ν_1 and ν_3 shown in Fig. 2. The absence of $N - N$ tunneling splitting in $N_2 - DOH$ and in the ν_1 region in $N_2 - D_2O$ strongly suggests that the additional tow-fold tunneling splitting in the ν_3 bands is due to accidental degeneracies with dark states and not because of ν_3 intramolecular excitation lowering the potential energy barrier between minima on the PES.

From the comparison between the $O - D$ asymmetric stretch $K_a = 0 \leftarrow 0$ band of the $N_2 - DOH$ and $N_2 - D_2O$ complexes and the discussion above, we can conclude that the ν_3 vibrational state is highly perturbed by an intermolecular mode combined with the ν_1 vibrational state and that this mode promotes significant $N - N$ tunneling motion.

Intramolecular dynamics and the vibrational shifts

Band-origins of the tunneling states in the ν_1 and ν_3 vibrational excited states of the $N_2 - D_2O$ complex have been obtained. The averaged band-origins of the complex were redshifted by only 0.629 cm^{-1} and 1.811 cm^{-1} from that of the D_2O monomer, respectively[42]. The band-origin of the $N_2 - DOH$ complex in the ν_1 vibrational excited state has a

redshift of 3.042 cm^{-1} from that of isolated DOH[49].

Concerning the vibrational shift in ν_2, Wang and Carrington Jr[20] concluded that: "about 75% of the band center shift is due to the change of the rotational constant of the monomer. The other 25% must be due to the change of the potential energy surface." Analyzing our results in the light of their work and assuming the same proportion for the two different mechanisms, the value of the vibrational shift that accounts for the change of the potential energy surface due to excitation of ν_3 mode is 0.453 cm^{-1}, indicating a small effect on the intermolecular dynamics of the $N_2 - D_2O$ complex and on the intramolecular vibration of the asymmetric stretch of D_2O.

V. CONCLUSION

The rovibrationally resolved spectra of the $N_2 - D_2O$ complex in the symmetric ν_1 and asymmetric ν_3 stretch regions of D_2O have been recorded and analyzed. The analysis was made by taking into account the large amplitude motions occurring in the complex : $D - D$ and $N - N$ exchange tunnelings. The structure of the energy levels and the tunneling splittings in the excited ν_1 and ν_3 vibrational states are reported. These splittings increases significantly upon the intramolecular ν_3 vibrational excitation but not on the intramolecular ν_1 vibrational excitation indicating that the bands in the ν_3 region are perturbed by a combination of state that includes ν_1 excitation and multiple excitation of the intermolecular N_2 bending modes. Further theoretical studies might identify the dark state and future experimental work in the overtone range where the density of states is increased could bring light on the accidental nature of this observation. The vibrational shifts indicates a negligible effect of the excited state on the intermolecular dynamics. Finally, a lower limit for the binding energy $D_0 = 120$ cm^{-1} was determined from observation of discrete perturbations.

ACKNOWLEDGMENTS

The authors would like to thank X.-G. Wang and T. Carrington Jr. for sharing their results. They also thank A.R.W. McKellar for his insight and helpful comments in interpreting the results.

This work was funded by the Action de Recherches Concertées (Grant No. ARC iBEAM-18/23-090). R.G. is a FRIA grantee of the Fonds de la Recherche Scientifique (FNRS). A. J. B. and N. M.-A. acknowledge the Natural Sciences and Engineering Research Council of Canada for its financial support.

DATA AVAILABILITY

The data that support the findings of this study are either avail- able from the supplementary material[41] or from the corresponding author upon reasonable request.

REFERENCES

[1] P. Chỳlek and D. Geldart, "Water vapor dimers and atmospheric absorption of electromagnetic radiation," Geophysical research letters **24**, 2015–2018 (1997).
[2] H. G. Kjaergaard, T. W. Robinson, D. L. Howard, J. S. Daniel, J. E. Headrick, and V. Vaida, "Complexes of importance to the absorption of solar radiation," The Journal of Physical Chemistry A **107**, 10680–10686 (2003).
[3] V. Vaida, K. J. Feierabend, N. Rontu, and K. Takahashi, "Sunlight-initiated photochemistry: Excited vibrational states of atmospheric chromophores," International Journal of Photoenergy **2008** (2008).
[4] V. Vaida, "Perspective: Water cluster mediated atmospheric chemistry," The Journal of chemical physics **135**, 020901 (2011).
[5] N. S. Shuman, D. E. Hunton, and A. A. Viggiano, "Ambient and modified atmospheric ion chemistry: From top to bottom," Chemical reviews **115**, 4542–4570 (2015).
[6] I. M. Svishchev and R. J. Boyd, "Van der waals complexes of water with oxygen and nitrogen: Infrared spectra and atmospheric implications," The Journal of Physical Chemistry A **102**, 7294–7296 (1998).
[7] J. S. Daniel, S. Solomon, H. G. Kjaergaard, and D. P. Schofield, "Atmospheric water vapor complexes and the continuum," Geophysical research letters **31** (2004).
[8] P. Demontis, A. Gamba, B. Manunza, and G. Suffritti, "An intermoleeular potential function for the n2- h2o system from ab initio mo calculations," Molecular Physics **47**, 347–354 (1982).
[9] L. Curtiss and C. Eisgruber, "A theoretical study of the interaction of n2 with water molecules.(h2o) n: N2, n= 1–8." The Journal of chemical physics **80**, 2022–2028 (1984).
[10] D. B. Kitchen, T. P. Ruane, and L. C. Allen, "Water binding in cryogenic liquids: The h2o… n2 hydrogen bond," Chemical physics letters **141**, 525–529 (1987).
[11] P. Sandler, J. O. Jung, M. Szczęśniak, and V. Buch, "The complex of n2 with h2o, d2o, and hdo: a combined ab initio and diffusion monte carlo study," The Journal of chemical physics **101**, 1378–1391 (1994).
[12] K. A. Franken and C. E. Dykstra, "Quantum monte carlo vibrational analysis of the nitrogen-water complex," Chemical physics letters **220**, 161–166 (1994).
[13] T. Mokomela, I. Rencken, G. Yeo, and T. Ford, "Ab initio molecular orbital calculations of the infrared spectra of interacting water molecules part 2. complexes of water with carbon monoxide and nitrogen," Journal of molecular structure **275**, 33–54 (1992).
[14] J. Sadlej, B. Rowland, J. Devlin, and V. Buch, "Vibrational spectra of water complexes with h2, n2, and co," The Journal of chemical physics **102**, 4804–4818 (1995).
[15] H. G. Kjaergaard, G. R. Low, T. W. Robinson, and D. L. Howard, "Calculated oh-stretching vibrational transitions in the water- nitrogen and water-oxygen complexes," The Journal of Physical Chemistry A **106**, 8955–8962 (2002).
[16] A. S. Tulegenov, R. J. Wheatley, M. P. Hodges, and A. H. Harvey, "Intermolecular potential and second virial coefficient of the water-nitrogen complex," The Journal of chemical physics **126**, 094305 (2007).
[17] P. R. Barreto, A. F. Albernaz, A. Capobianco, F. Palazzetti, A. Lombardi, G. Grossi, and V. Aquilanti, "Potential energy surfaces for interactions of h2o with h2, n2 and o2: A hyperspherical harmonics representation, and a minimal model for the h2o–rare-gas-atom systems," Computational and Theoretical Chemistry **990**, 53–61 (2012).
[18] Y. I. Baranov, I. Buryak, S. Lokshtanov, V. Lukyanchenko, and A. Vigasin, "H2o- n2 collision-induced absorption band intensity in the region of the n2 fundamental: ab initio investigation of its temperature dependence and comparison with laboratory data," Philosophical Transactions of the Royal Society A: Mathematical, Physical and Engineering Sciences **370**, 2691–2709 (2012).
[19] T. L. Ellington and G. S. Tschumper, "Anchoring the potential energy surface of the nitrogen/water dimer, n2⋯ h2o, with explicitly correlated coupled-cluster computations," Computational and Theoretical Chemistry **1021**, 109–113 (2013).
[20] X.-G. Wang and T. Carrington Jr, "The vibration-rotation-tunneling levels of n2–h2o and n2–d2o," The Journal of chemical physics **143**, 024303 (2015).

[21] L. Wang, X.-L. Zhang, Y. Zhai, M. Nooijen, and H. Li, "Explicitly correlated ab initio potential energy surface and predicted rovibrational spectra for h2o–n2 and d2o–n2 complexes," The Journal of Chemical Physics **153**, 054303 (2020).

[22] H. O. Leung, M. D. Marshall, R. Suenram, and F. Lovas, "Microwave spectrum and molecular structure of the n2–h2o complex," The Journal of chemical physics **90**, 700–712 (1989).

[23] P. A. Stockman, *Microwave and far-infrared spectroscopy of water-containing, hydrogen-bonded dimers: vibrational, rotational, and tunneling dynamics*, Ph.D. thesis, California Institute of Technology (1996).

[24] S. Springer, B. McElmurry, Z. Wang, I. Leonov, R. Lucchese, J. Bevan, and L. Coudert, "Rovibrational analysis of the water bending vibration in the mid-infrared spectrum of atmospherically significant n2–h2o complex," Chemical Physics Letters **633**, 229–233 (2015).

[25] Y. Zhu, R. Zheng, S. Li, Y. Yang, and C. Duan, "Infrared spectra and tunneling dynamics of the n2–d2o and oc–d2o complexes in the ν 2 bend region of d2o," The Journal of chemical physics **139**, 214309 (2013).

[26] A. Barclay, A. van der Avoird, A. McKellar, and N. Moazzen-Ahmadi, "The water–carbon monoxide dimer: new infrared spectra, ab initio rovibrational energy level calculations, and an interesting in-termolecular mode," Physical Chemistry Chemical Physics **21**, 14911–14922 (2019).

[27] S. Kuma, M. N. Slipchenko, K. E. Kuyanov, T. Momose, and A. F. Vilesov, "Infrared spectra and intensities of the h2o and n2 complexes in the range of the ν1-and ν3-bands of water," The Journal of Physical Chemistry A **110**, 10046–10052 (2006).

[28] A. Gutberlet, G. Schwaab, and M. Havenith, "High resolution ir spectroscopy of hdo and hdo (n 2) n in helium nanodroplets," The Journal of chemical physics **133**, 154313 (2010).

[29] L. Andrews and S. R. Davis, "Ftir observation of n≡ n stretching fundamentals in hydrogen-bonded complexes in solid argon," The Journal of chemical physics **83**, 4983–4989 (1985).

[30] S. Coussan, A. Loutellier, J. Perchard, S. Racine, and Y. Bouteiller, "Matrix isolation infrared spectroscopy and dft calculations of complexes between water and nitrogen," Journal of molecular structure **471**, 37–47 (1998).

[31] S. Hirabayashi, K. Ohno, H. Abe, and K. M. Yamada, "Infrared spectra of the water-nitrogen complexes (h 2 o) 2–(n 2) n (n= 1–4) in argon matrices," The Journal of chemical physics **122**, 194506 (2005).

[32] W. Hujo, M. Gaus, M. Schultze, T. Kubar, J. Grunenberg, M. Elstner, and S. Bauerecker, "Effect of nitrogen adsorption on the mid-infrared spectrum of water clusters," The Journal of Physical Chemistry A **115**, 6218–6225 (2011).

[33] D. Cappelletti, P. Candori, L. F. Roncaratti, and F. Pirani, "A molecular beam scattering study of the weakly bound complexes of water and hydrogen sulphide with the main components of air," Molecular Physics **108**, 2179–2185 (2010).

[34] Z. Abusara, L. Borvayeh, N. Moazzen-Ahmadi, and A. McKellar, "Isotope effects in the infrared spectra of ocs–he complexes and clusters," The Journal of chemical physics **125**, 144306 (2006).

[35] J. Norooz Oliaee, M. Dehghany, N. Moazzen-Ahmadi, and A. McKellar, "Fundamental and torsional combination bands of two isomers of the ocs–co2 complex in the co2 ν3 region," The Journal of Physical Chemistry A **117**, 9605–9611 (2013).

[36] L. Coudert and J. Hougen, "Tunneling splittings in the water dimer: Further development of the theory," Journal of Molecular Spectroscopy **130**, 86–119 (1988).

[37] J. K. Watson, "Determination of centrifugal distortion coefficients of asymmetric-top molecules," The Journal of Chemical Physics **46**, 1935–1949 (1967).

[38] J. K. Watson, *Vibrational Spectra and Structure*, j. durig ed., Vol. 6 (Elsevier, Amsterdam, 1977) p. 1.

[39] C. M. Western, "Pgopher: A program for simulating rotational, vibrational and electronic spectra," Journal of Quantitative Spectroscopy and Radiative Transfer **186**, 221–242 (2017).

[40] K. Yamada and M. Winnewisser, "Comments on quartic centrifugal-distortion constants for asymmetric-top molecules," Z Naturforsch A **31**, 131–138 (1976).

[41] See supplementary materials for observed transitions and splittings.

[42] J. Tennyson, P. F. Bernath, L. R. Brown, A. Campargue, A. G. Császár, L. Daumont, R. R. Gamache, J. T. Hodges, O. V. Naumenko, O. L. Polyansky, *et al.*, "Iupac critical evaluation of the rotational–vibrational spectra of water vapor. part iv. energy levels and transition wavenumbers for d216o, d217o, and d218o," Journal of Quantitative Spectroscopy and Radiative Transfer **142**, 93–108 (2014).

[43] X.-G. Wang and T. Carrington Jr., private communication.

[44] A. McKellar, Y. Zeng, S. Sharpe, C. Wittig, and R. Beaudet, "Infrared absorption spectroscopy of the co- ar complex," Journal of Molecular Spectroscopy **153**, 475–485 (1992).

[45] T. Hu, D. G. Prichard, L. H. Sun, J. Muenter, and B. Howard, "The vibration-rotation spectrum of the argon-acetylene van der waals complex," Journal of Molecular Spectroscopy **153**, 486–496 (1992).

[46] C. Lauzin, L. H. Coudert, M. Herman, and J. Liévin, "Ab initio intermolecular potential of ar–c2h2 refined using high-resolution spectroscopic data," The Journal of Physical Chemistry A **117**, 13767–13774 (2013).

[47] C. H. Townes and A. L. Schawlow, "Microwave spectroscopy," (McGraw-Hill Book Company, New-York, 1955) pp. 83–87.

[48] P. R. Bunker and P. Jensen, *Molecular symmetry and spectroscopy*, e-book ed. (NRC Research Press, Ottawa, Ontario, Canada, 2012) 748 p.

[49] J. Tennyson, P. F. Bernath, L. R. Brown, A. Campargue, A. G. Csaszar, L. Daumont, R. R. Gamache, J. T. Hodges, O. V. Naumenko, O. L. Polyansky, *et al.*, "Iupac critical evaluation of the rotational–vibrational spectra of water vapor. part ii: Energy levels and transition wavenumbers for hd16o, hd17o, and hd18o," Journal of Quantitative Spectroscopy and Radiative Transfer **111**, 2160–2184 (2010).